International Journal of Catalysis and Chemical Engineering

PRIME OPEN ACCESS

Volume 1, Issue 2

Research Article

Date of Submission: 18 April, 2025
Date of Acceptance: 24 July, 2025
Date of Publication: 06 August, 2025

Balancing Energy Efficiency and Biomass Yield Through Computational Fluid Dynamics of a Commercial Scale Bubble-Column Photobioreactor

Kubelka, B. G[1,2,3*], Abreu, P. C.[1] and Pinto, W. T[2]

[1]Laboratory of Microalgae Production – Institute of Oceanography – Federal University of Rio Grande, Rio Grande, Brazil

[2]Laboratory of Fluid Structure Interaction – Engineering School – Federal University of Rio Grande, Rio Grande, Brazil

[3]AlgaSul Biotecnologia de Microalgas – Oceantec – Technological Park - Federal University of Rio Grande, Rio Grande, Brazil

***Corresponding Author:**
Kubelka, B. G, Laboratory of Microalgae Production – Institute of Oceanography – Federal University of Rio Grande, Rio Grande, Brazil.

Citation: Kubelka, B. G., Abreu, P. C., Pinto, W. T. (2025). Balancing Energy Efficiency and Biomass Yield Through Computational Fluid Dynamics of a Commercial Scale Bubble-Column Photobioreactor. *Int J Catalysis Chem Eng, 1*(2), 01-12.

Abstract
Microalgae biomass derived fuel need to maximize production with minimal energy input to cultivation and harvesting operations. The mixing/circulation comprises an essential step in the expensive microalgae cultivation process. Additionally, prevents cell settlement and increases exposure to light and nutrients. Nevertheless, it is responsible for at least one-third of total cost to produce lipid from microalgae. Regulating air input is an effective way to save energy, but it can compromise production. Computational Fluid Dynamics was used to determine the percentage of dead-zones in 330 L photobioreactors (aspect ratio of 4.54) for production of the microalgae Nannochloropsis oceanica with different airflow. Three numerical cases were selected for growth experiments. The airflow rate of 0.0024 vvm allowed satisfactory production and low energy input. It is noteworthy that experiments with the highest Energy Return On Investment values were also observed in this airflow rate (0.0024 vvm). The complementary application of the tools (Energy Return on Investment and Computational Fluid Dynamics) have shown high potential to reach the economic viability of microalgae biofuel.

Keywords: Microalgal biofuel, Computational Fluid Dynamic, Energy Return on Investment, Efficient Mixing, Large-Scale, Viable Biomass

Introduction
The society is eagerly looking for economically viable bioenergetic solutions to the near future limited supply of fossil fuel. Plant biomass derived fuel need to maximize production with minimal energy input to cultivation and harvesting operations. Microalgae present several key advantages over higher plants as renewable source of sustainable biofuel [1]. Nevertheless, inevitably there is a demand for successful advances in cultivation tank design, so it can also be scaled up with more reduced cost and that has attracted the interest of several groups [2-4]. Of the entire microalgae biomass production chain, about 27% of the total cost are due to the energy consumption by the culture tank mixing/circulation system [5]. Despite the importance of other variables like culture media, light, temperature and pH, the adequate control of the airflow rate could enable a favorable balance between energy cost and microalgae biomass production [6].

Decreasing airflow rate in the cultivation tank results in a marked reduction in the surface velocity of air getting into the culture tank [7]. This may result in higher settling of microalgae cells forming dead-zones, and leading to a decrease in biomass productivity [8,4]. On the other hand, low airflow rate leads to a reduction in the energy cost to

produce microalgae biomass [9]. The application of the Energy Return on Investment (EROI) analysis allows accurately establishing a proper equilibrium between productivity and energy-saving. Additionally, it is an opportunity to compare with other energy sources [10]. Values of EROI greater than 1.0 indicate the economic potential of an energy source as an adequate substitute for fossil fuel. For instance, gasoline presents an Energy Return on Investment between 5.0 and 10.0 [11,10]. Bioenergy sources stand back with values of 0.42 in the EROI analysis performed in a microalgae cultivation raceway and 0.8 from terrestrial plants [12,10].

Biofuel from microalgae biomass have low EROI values, compared to fossil fuel, mainly due to the lack of adequate energy-efficiency improvements in the cultivation systems. Most of the reported improvements addresses increasing productivity only but rarely consider the most adequate cost-benefits of the system [13]. The economic viability of a microalgae biofuel plant stands on producing the most, consuming minimum energy and low-cost cultivation resources [14-16]. In this context, the Microalgae Production Laboratory (LPM) at the Federal University of Rio Grande, works in the development of a low-cost biomass production system. To achieve this, the laboratory began seeking methods to improve cultivation conditions without increasing energy requirements or indeed reducing production costs [4,17,18]. Harvesting procedures also were developed by LPM so biomass production costs were also reduced [19].

Currently, LPM uses 330 L (aspect ratio = 4.54 – see Table 1) bubble column photobioreactors (PBR) to produce massive volumes of an oil rich marine microalga, Nannochloropsis oceanica. These vertical tubular PBR, used by LPM, after appropriate productivity and energy-efficiency improvements show high potential for commercial scale up for biofuel production. This is principally, because of the simplicity and the easiness of reproducibility of the tank and the air-injection system, which have been pointed out as the most critical barriers in the proper use of PBR to commercial microalgae biomass production [20]. However, improvements can be pursued by employing Computational Fluid Dynamics (CFD) which saves valuable time and prolonged effort including cost in constructing several PBR air-injection systems and successive experimental procedures.

D (m)	h (m)	V (m^{-3})	N_{Inj}	D_{Inj} (mm)	D_{bm} (mm)
0.55	1.25	0.33	9	1	6.5

Table 1: Dimensions of the Closed Cylindrical Bubble Column Photobioreactor (PBR) and the Nozzle the Installed in the PBR

Previously, studies developed in our laboratory have already improved productivity without an increase in energy consumption in these PBR through the reduction of air nozzles sizes and, consequently improving mixing condition inside PBR [4,21]. Naturally, the next step consists of optimizing the volume of air supplied, so there is no energy waste by the air blower. Simultaneously to the use of CFD, the Energy Return on Investment (EROI) analysis was implemented to assess the influence of increased efficiency in microalgae biomass production and its energy-cost in the context of biofuel production.

In the present study, in silica analysis of the different airflow rates and its potential maximization in the PBR production of N. oceanica is presented. The validity of the CFD results was checked by cultivation experiments. Furthermore, the EROI analysis was carried out to estimate the energy-efficiency of three airflow rates chosen through the CFD tool as most effective air injection configuration.

Material and Methods

Computational Fluid Dynamics Simulations

Geometry and Computational Mesh

The computational geometry is a reproduction of the experimental bubble column photobioreactor in the Microalgae Production Laboratory (LPM) at the Federal University of Rio Grande (FURG). Figure 1 A shows the experimental setup at LPM/FURG and Figure 1 B the numerical representation developed in the 3D CAD tool of the CFD program STAR-CCM+ 14.09. The single air nozzle installed in tank's bottom is composed by nine 1mm orifices (air injectors). See Table 1 and for the 330 L PBR and air injection system design details [4].

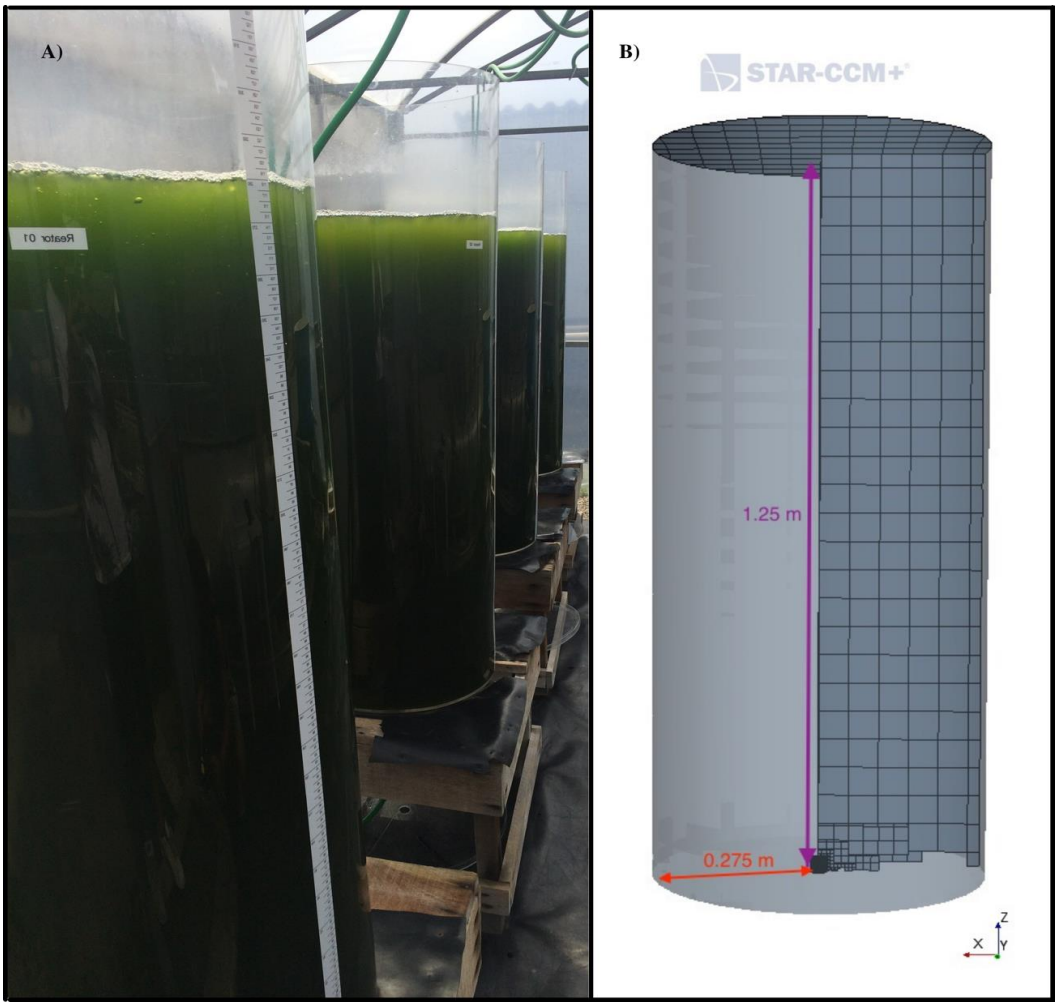

Figure 1: Bubble Column Photobioreactor of 330 L Used in this Study at the Microalgae Production Laboratory in the Federal University of Rio Grande, Brazil. A) Experimental Configuration; b) Computational Geometry and Mesh (Pink Arrow Highlights the Tank Height and Red Arrow Tank Radius)

Computational mesh development was done within STAR-CCM+. Mesh characteristics are found in Table 2 and in more detail in the work done by [4]. Mesh quality is secured by running Mesh Diagnosis. Another tool included in the CFD software [22]. This tool evaluates the mesh face validity, volume change and skewness angle as shown in Table 2.

NC	MCS	FV	VC	SA
0.55	1.25	0.33	9	1

Table 2: Mesh Description of the Simulated Cases

Initial and Boundary Conditions

With the progress of simulation, the air enters the bottom of the tank through a nozzle consisting of nine 1mm air injectors. A degassing condition (air outlet) was set to the upper wall of the Photobioreactor (PBR). The tank walls do not allow air or water out. Airflow rate adjustment (Q) was numerically controlled by the initial air velocity (U), which is calculated from Equation 1 and the calculations of the initial velocity conditions are in Table 3.

Case	Q (*vvm*)	U (m s^{-1})	DZ (%)
1	0.0012	0.105	86.25
2	0.0024	0.210	77.49
3	0.0082	0.720	75.55
4	0.0170	1.470	74.12
5	0.0242	2.100	73.82

Table 3: CFD Simulations Initial Conditions and Results for All Cases Numerically Studied. Q goes to the Airflow Rate, U is the Air Velocity Inlet to the Simulations Correspondent to Q and DZ is the Volumetric Percentage of Dead Zones

$$U = \frac{Q}{A} \qquad \text{Equation 1}$$

Where A is the sum of the area of the air bubble injectors?

Physical Models

Air-water interactions within the culture tank were considered multiphase problems, where air momentum is transferred to water. To predict the circulation of water resulting from the injection of air into the water tank the multiphase segregated flow model was solved with a set of conservation equations for each Eulerian phase. First order temporal discretization with a time step equal to $5.0E^{4}$ was used and the convection velocity was adjusted to second order. The Solver simple algorithm was applied to control the general solution [22]. When each phase solution is completed, phase interaction models (Eulerian Multiphase) are used to define the influence that one phase has on another in the interfacial area between them [22].

Hydrodynamic Considerations to Mixing Improvements

The photobioreactors of the Laboratory of Microalgae Production has a bubbling column mixing system, where the air enters at the bottom and center of the tank. After bubbles entering, it rises to the surface of the water and in the way up transfer momentum to water, resulting in a water circulation velocity. Dead-zones are created where this circulation velocities do not exceed the settling velocity. created a Stoke`s law based optimizing methodology to reduce microalgae cultivation tanks dead-zones, that considers the characteristic of the species cultivated in the bubble column PBR to reduce dead-zones in the microalgae culture tanks. The dead-zones of Nannochloropsis oceanica can be avoided by velocities in the water column above $2.06E^{-6}$ ms^{-1} [4]. This theoretical settling velocity of *N. oceanica* was compared with the one second average field velocity for the entire volume of the tank. From this comparison, we determined the volume of dead-zones (V_{DZ}) and knowing the tank volume (V_T - Table 1) is possible to determine the percentage of dead-zones (DZ) in the tank as follows (Equation 2):

$$DZ = \frac{V_{DZ}}{V_T} \qquad \text{Equation 2}$$

The simulation time used for the analysis of dead-zones was randomly selected after the execution of 50 s (the simulation presented convergence after 30 s). In each case analyzed, a percentage of dead-zones (DZ) were determined. DZ was used as an improvement variable to select the cases to be tested experimentally.

Cultivation Methods

Culture Conditions

The microalgae specie used in cultivation experiments was Nannochloropsis oceanica (Eustigmatophyceae), cultivated in natural seawater (salinity varied according to the time of the year and the climate-Table 4) and filtered through polypropylene filters of 1.0 µm. After filtration, sodium hypochlorite at 12% (0.15 ml L-1) was added and after 24 hours it was neutralized with ascorbic acid [23]. A fertilizer-based medium was added at the beginning of the experiment and consisted of ammonium sulfate (150.0 mg L^{-1}), Urea (7.5 mg L^{-1}) and calcium superphosphate (25.0 mg L^{-1}) [18]. The tanks were placed in external agricultural greenhouses, so that the irradiance and photoperiod were natural (Table 4). The positioning of the photobioreactors was planned to mitigate the shading between the tanks, so the incident light was equal for each tank (Table 4). Temperature, light and pH were not controlled, although were measured every day as showed shown in Table 4. Temperature and pH were measured with a multiparameter 556 MPS (YSI) and the irradiance sensor LI-192 Underwater Quantum Sensor (LI-COR) was used. Samples of all analyzed variables were collected well in the center of the tank to guarantee a well-mixed culture sample.

Exp.	Date/season	Q (*vvm*)	T (˚C)	pH	S	L_{Sup}
1	13th – 25th Dec. 2017 (Austral summer)	0.0024	28.94 ± 3.66 22.75 – 35.50	9.45 ± 0.59 7.69 – 9.89	20.07 ± 0.27 20.00 – 21.00	720.34 ± 370.54 179.50 – 1235.00
		0.017	29.44 ± 3.69 22.75 – 35.00	9.47 ± 0.64 7.58 – 9.93	20.21 ± 0.54 20.00 – 21.50	697.63 ± 337.07 230.20 – 1230.00
2	05th – 15th Jan. 2018 (Austral summer)	0.0024	33.75 ± 1.28 31.40 – 37.10	8.51 ± 0.39 7.45 – 9.05	33.85 ± 0.58 33.15 – 34.72	910.73 ± 168.41 555.30 – 1099.00
		0.017	33.51 ± 1.45 31.30 – 37.60	8.42 ± 0.40 7.49 – 9.02	33.89 ± 0.67 33.10 – 34.95	768.36 ± 216.66 457.30 – 1147.00

3	23th Jan. – 01st Feb. 2018 (Austral summer)	0.0024	32.17 ± 1.56 28.75 – 33.65	8.35 ± 0.39 7.37 – 8.65	22.03 ± 0.38 21.56 – 22.57	744.70 ± 273.03 269.35 – 930.35
		0.017	31.77 ± 1.61 28.35 – 33.65	8.31 ± 0.39 7.36 – 8.70	22.04 ± 0.40 21.68 – 22.63	779.93 ± 303.61 291.90 – 1.092.00
4	26th Mar. – 09th Apr. 2018 (End of austral summer)	0.0024	29.39 ± 5.44 20.45 – 30.75	9.40 ± 0.33 7.62 – 9.62	29.50 ± 0.5 28.30 – 30.00	735.81 ± 171.83 484.80 – 986.
		0.0012	29.35 ± 4.67 21.75 – 32.50	9.38 ± 0.29 7.69 – 9.59	29.55 ± 0.48 28.38 – 30.10	805.83 ± 170.03 480.55 – 940.80
5	04th – 14th May 2018 (Austral fall)	0.0024	29.90 ± 2.60 27.50 – 35.00	9.55 ± 0.25 8.79 – 9.73	30.50 ± 0.10 30.30 – 30.70	371.89 ± 193.28 216.65 – 665.00
		0.0012	29.95 ± 2.55 27.35 – 34.95	9.59 ± 0.28 8.74 – 9.73	30.40 ± 0.1 30.20 – 30.60	411.51 ± 277.28 214.60 – 879.65
6	24th – 14th May 2018 (Austral fall)	0.0024	29.55 ± 2.67 27.10 -34.00	9.50 ± 0.48 8.32 – 9.66	28.92 ± 0.22 28.70 – 29.14	381.09 ± 153.58 195.15 – 605.00
		0.0012	29.50 ± 2.55 27.12 – 34.15	9.52 ± 0.49 8.36 – 9.69	28.90 ± 0.21 28.69 – 29.12	401.59 ± 250.26 215.60 – 755.61

Table 4: Date, Season, mean ± SD, Minimum and Maximum Values of Temperature (T - °C), Salinity (S), pH and Surface Irradiance (L_{Sup}) Measured During Growth Experiments (Exp.) With the Marine Microalga Nannochloropsis Oceanica in 330 L Vertical Closed Cylindrical Photobioreactor (PBR) with the Corresponding Airflow Rate (Treatment) - Q

The air injection in each photobioreactor of 330 L was measured by rotameters (estimated error in 10%) and controlled by manually adjusted valves. Three airflow rate adjustments were chosen from results of simulation to be compared experimentally as shown in Table 4. Four photobioreactors were used in each experiment, two for each air flow rate treatment, and the experiments were repeated in time. Therefore, three experiments for each comparison, enumerated next, were evaluated: i) Intermediate airflow rate (0.0024 vvm) vs. High airflow rate (0.017 vvm); ii) Low airflow rate (0.0012 vvm) vs. Intermediate airflow rate (0.0024 vvm).

The microalgae biomass was determined by dry weight measurements of algae concentrated in 0.7 µm (GF/F) pre-weighted fiberglass filters and washed with 0.65 M ammonium formiate (10 ml) to remove the absorbed salt, according to [14]. Additionally, the biomass gain/loss on the last day of cultivation were compared between treatments. The calculation of biomass gains or loss (B_g - %) was as follows in Equation 3:

$$B_g = \left(\frac{B_{y_I} - B_{y_{L\,or\,H}}}{B_{y_{L\,or\,H}}}\right) \times 100 \qquad \text{Equation 3}$$

Where B_y is the biomass yield, determined by subtracting the final from initial biomass, for each treatment? For instance, B_{y_I} corresponds to the biomass yield of intermediate airflow rate, B_{y_L})and B_{y_H} are the biomass yield for low and high airflow rates, respectively.

Statistical Analysis

First, the data were tested for normality (Shapiro-wilk test) and homoscedasticity (Levene test). Subsequently, these assumptions were satisfied, the significance of the differences between the biomass of the two mixing conditions (airflow rate) was determined through a repeated measure analysis of variance (ANOVA). A confidence interval of 95% was considered for the significance tests [24]. All graphic representations were developed with Graphpad Prism 7. All charts were plotted by the average value of the data, and the error bars are shown to represent the standard deviations.

Also, in the software Graphpad Prism 7, a non-linear regression analysis is tested between the airflow rates numerically simulated and the resulting dead-zones predicted. Exponential one phase decay equation model is applied to fit the data analyzed as described by Equation 4 [25].

$$Y = (Y_0 - p) * exp(-K * X) + p \qquad \text{Equation 4}$$

Where Y_0 is the Y value (dead-zones) when X (airflow rate) is zero, p is the Y value in infinite time and K is the rate constant.

Energy Efficiency Analysis

The EROI (Energy Return on Investment) method is the ratio between the energy taken from the fuel that could be used (P_{out}) and the energy invested to produce this fuel (P_{in}), as described in Equation 5.

$$EROI = \frac{P_{out}}{P_{in}} \qquad \text{Equation 5}$$

An estimation of energy production from the lipid content of microalgae (P_{out}) can be calculated from the volumetric rate of lipid productivity (L – Equation 6). The present study did not perform analysis of lipid content. Therefore, we used the data of other work developed in the Laboratory of Microalgae Production at FURG. From the work of and from laboratory daily routines analyses we defined a seasonal average of 30% of the dry weight of saponifiable lipids, which are the lipids transformed in biofuel [26,27]. From these values and the result from cultivation experiments it proved possible to estimate value.

$$L = \frac{B_f f - B_i f_i}{\Delta t} \qquad \text{Equation 6}$$

Where B_f is the microalgae biomass determined on the last day of the cultivation experiments, B_i corresponds to biomass on the day of the beginning of the experiments, f and f_i are the final and initial lipid, respectively (30% of the final and initial biomass dry weight). And Δt is the cultivation time for each batch.

By applying the volumetric rate of lipid productivity (L) in Equation 6, an estimative of the energy generation from the lipids produced from the biomass of N. oceanica, P_{out} (Wm^{-3}), was determined in Equation 7, as also described by [6].

$$P_{out} = 0.0116\, L\, \Delta G \qquad \text{Equation 7}$$

Where ΔG is the energy contained in lipid, which is equal to 38,390 J.

The next step of EROI analysis was calculating the energy demand of the system of the LPM/FURG. Four stages for microalgae biofuel production are: i) cultivation; ii) harvesting; iii) lipid extraction; iv) transesterification. In the cultivation stage, the costs of pumping saltwater and culture are constant as the volume pumped in all experiments were the same – P_{pump} = 0.0825 Wm^{-3}. The regulation of air intake allows to compare different airflows rates (Q – treatments), and consequently different energy expenditures (P_{air} – Wm^{-3}), as can be observed in Equation 8.

$$P_{air} = \rho * g * u_g \qquad \text{Equation 8}$$

Where ρ is the density of the liquid (microalgae culture – 1036.00 $Kg.m^{-3}$), g is the gravitational acceleration and u_g is the superficial gas (air) velocity.

After cultivation comes the harvesting stage. Centrifugation is usually applied to separate saltwater from microalgae biomass [14]. However, the Laboratory of Microalgae Production (LPM–FURG) has been developing protocols that avoid the use of centrifugation to advance to the next step, the lipid extraction. Achieved high harvesting efficiency with flocculation in pilot scale conical settling tanks [19]. The product of this flocculation/settlement process is microalgae paste that has been used successfully by to extract lipids through the microwave method. Flocculation/settling process presents an energy cost related to the preparation of the flocculant (bench-top shaker) and homogenizing it with the culture (low velocity electric motor attached to a paddlewheel) – P^{floc} = 0.0130+0.045 = 0.058 Wm^{-3} [26].

The energy expenditure of the microwave lipid extraction method was determined according to descriptions of energy spent to extract lipid from 1 kg of microalgae paste [26]. This value was used to calculate how much energy would be spent to extract 330 L of each paste concentrate for each experiment, P_{extr} . Finally, the fourth stage to generate biofuel, the transesterification process, where grossly the lipid is transformed to biofuel. The supercritical transesterification method is the most applied by our working partners. This method was estimated by to have an energy input of Ptrans = 1,365 Wm-3 [28]. All these energy inputs were added to account for the calculation of the P_{in}, which is used in Equation 4 to determine the EROI values for each experiment carried out in the present study.

Results and Discussion

Air Injection Hydrodynamic Performance

The numerical simulation of five airflow rates resulted in distinct values of dead-zones (DZ) inside the 330 L bubble column PBR as showed in Table 3. Higher volume of DZ is observed in Case 1, adjusting air injection with lower airflow rate (0.0012 vvm). When doubling this airflow rate, as in Case 2, DZ values decreased 8.76 pp (percentage points). Differently, from Case 2 to 5, a slight variation was estimated in DZ. For a specific example, from Case 3 (0.0082 vvm) to 4 (0.0170 vvm), that is doubling the airflow rate, we noted a modest decrease in dead-zones by just 1.43 pp. Therefore, an interesting relationship between airflow rate and dead-zones percentage was drawn in this study as shown in Figure 2. There is a non-linear relationship between these variables and an exponential decay pattern is supported by the R^2 value of 0.98.

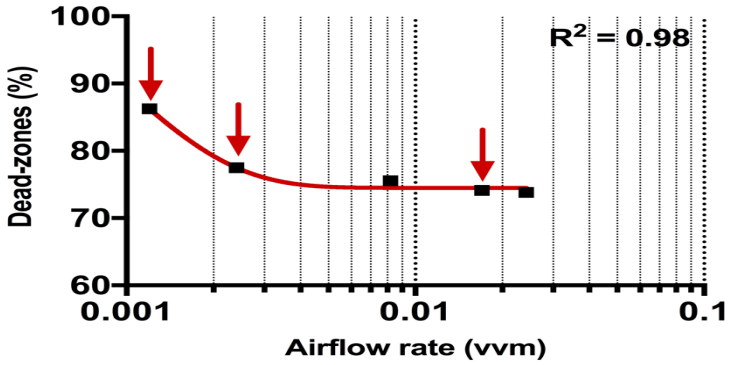

Figure 2: Non-Linear Regression Analysis for The Exponential Decay of The Influence of The Airflow Rate Over Dead-Zones Percentage (%). Note, In Red on The Adjusting Curve and At Top Right the Value of The R Square of The Adjusted Curve. The Red Arrow Indicates the Simulation Cases Performed Experimentally

As the values of the airflow rates are increased to 0.0024 vvm the momentum transfer from the injected air to adjacent water is suggested to be lost at the surface by bubble breakage, as superficial velocity is also increased by increasing air flow rate [7]. Increasing superficial air velocity may have several effects on the hydrodynamic performance of bubble column reactors. Observed that the mixing time decreases as the superficial gas velocity increases up to a threshold velocity value, increasing further authors observed that the mixing time changed little or none [8]. Authors refer that this may be due to the formation of many circulation loops. The effect suggested here is that airflow rate increase, and consequently, the higher value of superficial air velocity may cause the reduction in dead zones inside PBR only to a certain superficial gas velocity threshold value. That is 0.0024 vvm. Therefore, airflow-rate above 0.0024 vvm invariably is not so effective in reducing settlement of microalgae cells (dead-zones). More than that, it will be shown next that it represents an enormous increase in energy demand of the air supply system.

Based on the hydrodynamic investigation, particularly the percentages of dead-zones, and in the energy expenditure of the air injection system (Pair) as shown in Table 5, the three most promising cases were chosen for the experimental cultivation of microalgae. Energy input is directly proportional to the adjusted airflow rate, as described in Equation 7. The following criteria were carefully chosen to allow numerical results to be validated through growth experiments so that energy assessment analysis could be carried out: i) good hydrodynamic performance (Case 4); ii) lower energy demand (Case 1); iii) balance between energy efficiency and hydrodynamic performance (Case 2). This multidisciplinary approach is in accordance with what is argued by, that optimization of biomass production of microalgae should search to increase productivity, but as well to achieve cost reduction [29].

Exp./Q	P_{out} $(Wm^{-})^3$	P_{out} $(Wm^{-})^3$	P_{out} $(Wm^{-})^3$	P_{in} $(Wm^{-})^3$	P_{in} $(Wm^{-})^3$	P_{in} $(Wm^{-})^3$	EROI	EROI	EROI
	Low	*Interm.*	*High*	*Low*	*Interm.*	*High*	*Low*	*Interm.*	*High*
1	-	0.767	1.298	-	7.567	43.507	-	0.130	0.030
2	-	0.566	1.457	-	7.567	43.507	-	0.090	0.035
3	-	0.373	0.515	-	7.566	43.506	-	0.060	0.012
4	0.201	0.557	-	1.365	7.566	-	0.067	0.092	-
5	0.215	0.545	-	1.365	7.566	-	0.070	0.090	-
6	0.242	0.979	-	1.364	7.567	-	0.080	0.17	-

Table 5: Results of EROI Analysis for the Six Experiments (Exp.) of N. Oceanica Biomass Growth Subject to Different Airflow Rates (Treatments - Q). Low Goes to the Low Airflow Rate, Interm. is the Intermediate Airflow Rate and High the High air Flow rate? Also, the Variable of Power Input (Pin) and of the Output (P_{out}) is Shown

Biomass Production

Three specific cases of airflow rates selected (Cases 1, 2 and 4) by the criteria were compared, among themselves, in growth experiments of marine microalgae Nannochloropsis oceanica. Initially, three experiments were carried out to properly compare the biomass production between an air injection system with high airflow rate (0.0170 vvm - Case 4) and one with an intermediate airflow rate (0.0024 vvm - Case 2). Next, three other experiments compared a low airflow rate (0.0012 vvm - Case 1) with an intermediate airflow rate. The results of all six experiments for biomass production are illustrated in Figure 3 and in Table 6. It is noteworthy that the initial biomass of all six experiments showed no significant difference ($p>0.05$) among treatments (airflow rates).

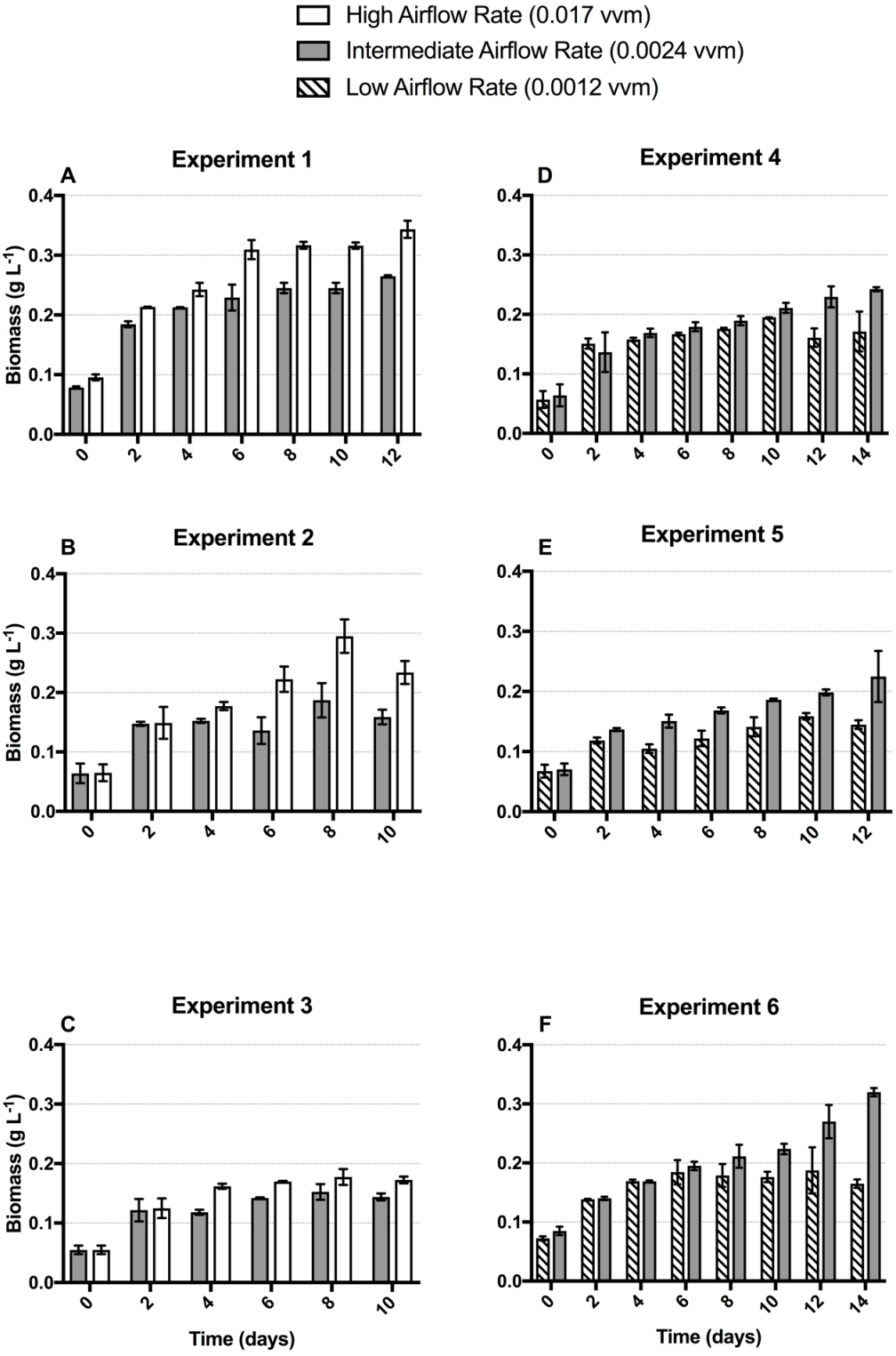

Figure 3: Average and Standard Deviation (n=2) of Biomass Production During the Six Growth Experiments with The Marine Microalgae Nannochloropsis Oceanica In Bubble Column Photobioreactors of 330 L. Three Airflow Rates were Studied: i) Low (Green) - 0.0012 Vvm; ii) Intermediate (Gray) - 0.0024 Vvm; iii) high (Blue) - 0.017 Vvm

Exp.	Q (*vvm*)	B_i (g L^{-1})	B_f (g L^{-1})	B_y (g L^{-1})	B_g (%)
1	0.0024 0.0170	0.079 ± 0.020 0.095 ± 0.049	0.265 ± 0.002 0.343 ± 0.014	0.186 ± 0.001 0.248 ± 0.019	- 33.14 ± 10.54
2	0.0024 0.0170	0.066 ± 0.017 0.064 ± 0.015	0.159 ± 0.012 0.234 ± 0.019	0.095 ± 0.004 0.168 ± 0.005	- 78.33 ± 12.87
3	0.0024 0.0170	0.055 ± 0.007 0.055 ± 0.007	0.144 ± 0.006 0.173 ± 0.011	0.089 ± 0.001 0.118 ± 0.018	- NS
4	0.0024 0.0012	0.064 ± 0.057 0.057 ± 0.018	0.243 ± 0.004 0.171 ± 0.034	0.179 ± 0.022 0.114 ± 0.019	- -48.64 ± 0.78
5	0.0024 0.0012	0.071 ± 0.010 0.068 ± 0.011	0.220 ± 0.049 0.145 ± 0.007	0.149 ± 0.040 0.078 ± 0.003	- -48.40 ± 13.22
6	0.0024 0.0012	0.085 ± 0.007 0.073 ± 0.004	0.320 ± 0.007 0.165 ± 0.007	0.235 ± 0.028 0.093 ± 0.011	- -60.43 ± 6.89

Table 6: Results of Dry Weight Measured in Growth Experiments with The Marine Microalga Nannochloropsis Oceanica in 330 L Vertical Closed Cylindrical Photobioreactor In the First Day of Cultivation (B_i) and in the Last (B_f). Also, the Yield (B_y) Was Determined Subtracting Final from Initial Biomass and The Gain/Loss (% - B_g) Was Calculated Comparing the Yields in All Airflow Rates. Loss Values Are Highlighted in Red (Negative). NS Stands for Not Significant Differences in The Biomass Production

In Figure 3 A (experiment 1) it is possible to observe a final biomass concentration of 0.265 ± 0.002 g L^{-1} for the treatment with intermediate airflow rate and 0.343 ± 0.014 g L^{-1} for the air injection system adjusted with a high airflow rate. This significant difference ($p>0.05$) represented a biomass gain of 33.14 ± 10.54% with the adjustment of a higher airflow rate. In experiment 2 (Figure 3 B), a biomass gain was also observed in the treatment with higher airflow rate over intermediate airflow rate (78.33 ± 12.87%). However, in experiment 3 (Figure 3 C), there was no significant difference ($p>0.05$) between the two adjusted airflow rates.

In Figures 3 D, E and F, the biomass concentration of the low airflow rate (0.0012 vvm) is compared with the intermediate airflow rate (0.0024 vvm). Significant differences emerged in the last day of cultivation of the experiments 4, 5 and 6. In experiment 4 (Figure 3 D) the intermediate airflow rate resulted in a final biomass production of 0.243 ± 0.003 g L-1 whereas in low airflow rate a final biomass of 0.149 ± 0.018 g L-1. Therefore, a loss (negative gain) of -48.64 ± 0.78% was observed in experiment 4 for the low airflow rate treatment in comparison to the intermediate airflow. Experiments 5 and 6 resulted in loss of biomasses of -48.40 ± 13.22% and -60.43 ± 6.89%, respectively. It is noteworthy, that a gain or a loss depends on which comparison is under analysis. As detailed in Equation 3, experiments with treatment of high airflow rate is compared to intermediate, resulting in loss of biomass. And, comparing low with intermediate airflow results in gain of biomass.

In the current work, experiments with three different airflow rates supported the results of the percentage of dead-zones (DZ) in simulations. In the lower airflow rate DZ volume was 8.75 pp. higher than the treatment of intermediate airflow rate, resulting an average biomass loss of 55%. In addition, comparison of the intermediate to the high airflow rates resulted in a decrease of 3.37 pp., where the higher airflow rate showed an average gain of 53% of biomass. However, comparisons performed adjusting the airflow rate to high (higher energy expenditure - Pair), apparently, would not compensate for the increment in biomass production. Taking together the biomass production the energetic balance between the production of lipids from this biomass of microalgae and the energy expenditure to produce this biomass.

Studied the microalgae growth in cultivation tanks [30]. The authors used a small volume (15.45 L) flat-plate photobioreactor to evaluate the hydrodynamic performance of four distinct airflow rates. As in our study, they found that increasing airflow rate may result in improved conditions to microalgae growth possibly due to increasing the water column mixture, preventing cells from settling and increasing the light-dark cycles [21,31,32]. Indeed, measured a high optical density value in the highest airflow rate adjusted by them [30]. However, optical density lacks in accuracy to estimate microalgae production, as different suspended particles can be measured [33]. Our numerical predictions showed that airflow rate adjusted too high may not improve microalgae cultivation conditions as observed by [30]. Additionally, the strategy to define ideal cultivation procedures relies on the cost-benefit of technology of microalgae production [34]. And, by using high airflow rates will not assure economic viability to biofuels produced from microalgae biomass.

Energy Efficiency of the Photobioreactor

The 24-hour functioning need of the air supply justifies the influence observed in the spent energy for air injection in the total energy costs (Pin) during PBR operation. The energy demand resulting of air injection (Pair) represented 71.9 % of Pin for the high airflow rate, by reducing the airflow rate to 0.0024 vvm (intermediate) represented only 27.0 % of the total cost of oil production, and low airflow rate represented 15.2 %. From this and from the previous analysis of the

biomass production it is already possible to have an indication of the airflow rate for greater efficiency (intermediate). Moreover, the incorporation of biomass production in the quantification of the best performance of each treatment of the air injection system makes the applicability of this strategy for the biofuels industry very valuable. It is worth mentioning that EROI analysis allows biofuels produced from microalgae to be compared with other fuels taking into account their energy efficiency.

A final analysis was carried out by applying an energy efficiency estimation tool, EROI (Energy Return on Investment) to our data. A microalgae cultivation system of 330 L closed cylindrical vertical photobioreactors was used. The estimation of the energy production from th e microalgae biomass (Pout - Equation 7 and Table 5) and the energy demand of the cultivation system (Pin - Equation 8 and Table 5) were used for the calculation of energy efficiency, as shown in Equation 5 - EROI.

Intermediate airflow rate resulted in ratein 48.03 ± 33.54 % increase in EROI value over the higher airflow rate. Higher final production (Figure 3 and Table 6), of the high airflow rate did not result in a higher energy efficiency. And, comparing the intermediate and the low airflow rates, a gain of 201.01 ± 55.08 % of energy efficiency was observed for the first one. Therefore, a solution to increase the viability of microalgae biofuel is related to balanced air injection, improving production without overwhelming energy expenditure by air injection system. This approach is in accordance with that proposed by [29].

Presented EROI values for a variety of energy sources, including renewable sources [10,11]. On the evaluations performed in the present study the intermediate airflow rate (adjusting a value of 0.0024 vvm) was considered more energy efficient, with an EROI = 0.309 ± 0.121, at least one order of magnitude below fossil fuel. Also, below solar panels (EROI = 1.2 – 1.8). Thus, it is suggested that there is economic viability (EROI > 1.0) in the use of Nannochloropsis oceanica biomass for industrial biofuel production [10]. However, this application still depends on the reduction of energy expenditure for the production of saponifiable lipids [35]. As well, systems that increase productivity without increasing energy expenditure, as achieved by and [36,4]. Furthermore, increase of lipid content throughout stressing methods and genetic engineering, as described by, may contribute to the increase of EROI values [37].

However, the value of the EROI of 0.31 still needs a series of improvements to establish a competitive production system with other fuel. It is noteworthy to mention a hybrid cultivation facility with photobioreactors and raceway tanks achieved EROI of 0.69 with the cultivation of freshwater microalgae species of Desmodesmus sp. We believe that the value of EROI achieved in the present work can be increased by other improvements in the air injection system, such as optimizing the distribution of air injectors at the bottom of the PBR and/or the conversion of the bubble column into an airlift by inserting a cylindrical baffle in the tank center. We have described here the optimization of microalgae cultivation in tanks based on CFD and EROI tools. Both applicative acted in synergy to balance energy expenditure and biomass production of Nannochloropsis. And by applying this optimization strategy for tanks, a viable microalgae production chain i suggested here, further supporting the approach as first proposed by [38].

Conclusions

The application of CFD to estimate dead-zones in synergy with EROI to estimate energy efficiency is a high potential strategy to make biofuel from microalgae a reality. In this study, a non-linear relationship between the airflow rate and the presence of dead-zones in the photobioreactors was established and an exponential decay pattern was observed on the curve between those two variables. Moreover, airflow rate adjustments allowed the reduction of the energy demand and maintained a satisfactory production [39]. However, there is still room for improvements in the marine microalgae cultivation methodology to reach EROIs comparable to those of fossil fuels.

Funding Declaration

B. Kubelka is a postdoctoral fellow from Fundação de Amparo à Pesquisa do Estado do Rio Grande do Sul (FAPERGS) (process number 23110.019930/2023-90) and P.C. Abreu was a research fellow of the National Councel of Technological and Scientific Development – CNPq. This study had financial support of the project Costs and productivity evaluation for massive microalgae cultivation for biodiesel production.

Competing Interest Declaration

There is no conflict of interest in current manuscript and all information produced here has the goal to enrich researching community.

Data Availability Declaration

No, I do not have any research data outside the submitted manuscript file.

References

1. Khan, M. I., Shin, J. H., & Kim, J. D. (2018). The promising future of microalgae: current status, challenges, and optimization of a sustainable and renewable industry for biofuels, feed, and other products. *Microbial cell factories, 17,* 1-21.
2. Posten, C. (2009). Design principles of photo-bioreactors for cultivation of microalgae. *Engineering in Life*

Sciences, 9(3), 165-177.
3. Salama, E. S., Kurade, M. B., Abou-Shanab, R. A., El-Dalatony, M. M., Yang, I. S., Min, B., & Jeon, B. H. (2017). Recent progress in microalgal biomass production coupled with wastewater treatment for biofuel generation. *Renewable and Sustainable Energy Reviews, 79*, 1189-1211.
4. Kubelka, B. G., Pinto, W. T., & Abreu, P. C. (2017). Hydrodynamic performance of two air nozzles diameters on the massive microalgae culture: Computational and experimental approaches. *Algal research, 27*, 318-324.
5. Pires, J. C., Alvim-Ferraz, M. C., & Martins, F. G. (2017). Photobioreactor design for microalgae production through computational fluid dynamics: A review. *Renewable and Sustainable Energy Reviews, 79*, 248-254.
6. Arudchelvam, Y., & Nirmalakhandan, N. (2012). Optimizing net energy gain in algal cultivation for biodiesel production. *Bioresource technology, 114,* 294-302.
7. Kulkarni, A. A., & Joshi, J. B. (2005). Bubble formation and bubble rise velocity in gas− liquid systems: a review. *Industrial & engineering chemistry research, 44*(16), 5873-5931.
8. Rampure, M. R., Kulkarni, A. A., & Ranade, V. V. (2007). Hydrodynamics of bubble column reactors at high gas velocity: experiments and computational fluid dynamics (CFD) simulations. *Industrial & Engineering Chemistry Research, 46*(25), 8431-8447.
9. Norsker, H., Barbosa, M. J., Vermuë, M. H., & Wijffels, R. H. (2012). On energy balance and production costs in tubular and flat panel photobioreactors. *TATuP-Zeitschrift für Technikfolgenabschätzung in Theorie und Praxis, 21*(1), 54-62.
10. Hall, C. A. S., Lambert, J. G., & Balogh, S. B. (2014). EROI of different fuels and the implications for society. *Energ Policy, 64,* 141-152.
11. Cleveland, C. (2005). Net energy from the extraction of oil and gas in the United States. *Energy, 30*(5), 769-782.
12. Beal, C. M., Stillwell, A. S., King, C. W., Cohen, S. M., Berberoglu, H., Bhattarai, R. P., ... & Hebner, R. E. (2012). Energy return on investment for algal biofuel production coupled with wastewater treatment. *Water Environment Research, 84*(9), 692-710.
13. Ho, S. H., Ye, X., Hasunuma, T., Chang, J. S., & Kondo, A. (2014). Perspectives on engineering strategies for improving biofuel production from microalgae--a critical review. *Biotechnol Adv, 32*(8), 1448-1459.
14. Borowitzka, M. A., & Moheimani, N. R. (Eds.). (2013). Algae for biofuels and energy (Vol. 5, pp. 133-152). Dordrecht: Springer.
15. Chua, E. T., & Schenk, P. M. (2017). A biorefinery for Nannochloropsis: Induction, harvesting, and extraction of EPA-rich oil and high-value protein. *Bioresour Technol, 244*(Pt 2), 1416-1424.
16. Slade, R., & Bauen, A. (2013). Micro-algae cultivation for biofuels: Cost, energy balance, environmental impacts and future prospects. *Biomass and Bioenergy, 53*, 29-38.
17. Kubelka, B. G., Roselet, F., Pinto, W. T., & Abreu, P. C. (2018). The action of small bubbles in increasing light exposure and production of the marine microalga Nannochloropsis oceanica in massive culture systems. *Algal Research, 35*, 569-576.
18. Faé Neto, W. A., Borges Mendes, C. R., & Abreu, P. C. (2018). Carotenoid production by the marine microalgae Nannochloropsis oculata in different low-cost culture media. *Aquaculture Research, 49*(7), 2527-2535.
19. Roselet, F., Burkert, J., & Abreu, P. C. (2016). Flocculation of Nannochloropsis oculata using a tannin-based polymer: Bench scale optimization and pilot scale reproducibility. *Biomass and Bioenergy, 87,* 55-60.
20. Seo, I.-h., Lee, I.-b., Hwang, H.-s., Hong, S.-w., Bitog, J. P., Kwon, K.-s., . . . Cuello, J. L. (2012). Numerical investigation of a bubble-column photo-bioreactor design for microalgae cultivation. *Biosystems Engineering, 113*(3), 229-241.
21. Neto, I. E. L., Zhu, D. Z., M.ASCE, & Rajaratnam, N. (2008). Air Injection in Water with Different Nozzles. *Journal of Environmental Engineering, 134*(4), 283-294.
22. Siemens. (2017). User Guide STAR-CCM+ v12.02. Retrieved from
23. Andersen, R. A. (Ed.). (2005). Algal culturing techniques. Academic press.
24. Zar, J. H. (2010). Biostatistical analysis: Prentice-Hall/Pearson.
25. Batschelet, E. (1971). Introduction to mathematics for life scientists (Vol. 2, pp. xiv+-495).
26. de Moura, R. R., Etges, B. J., dos Santos, E. O., Martins, T. G., Roselet, F., Abreu, P. C., . . . D'Oca, M. G. M. (2018). Microwave-Assisted Extraction of Lipids from Wet Microalgae Paste: A Quick and Efficient Method. *European Journal of Lipid Science and Technology, 120*(7).
27. Borges, L., Caldas, S., Montes D'Oca, M. G., & Abreu, P. C. (2016). Effect of harvesting processes on the lipid yield and fatty acid profile of the marine microalga Nannochloropsis oculata. *Aquaculture Reports, 4*, 164-168.
28. Montcho, P., Christian, K. T. R., Pascal, A. D. C., Assou, S., & Dominique, S. C. K. (2018). Comparative Study of Transesterification Processes for Biodiesel Production (A Review). Applied Chemistry, 120.
29. Hulatt, C. J., & Thomas, D. N. (2011). Energy efficiency of an outdoor microalgal photobioreactor sited at mid-temperate latitude. *Bioresour Technol, 102*(12), 6687-6695.
30. Yang, Z., del Ninno, M., Wen, Z., & Hu, H. (2014). An experimental investigation on the multiphase flows and turbulent mixing in a flat-panel photobioreactor for algae cultivation. *Journal of Applied Phycology, 26*(5), 2097-2107.
31. Gao, X., Kong, B., & Dennis Vigil, R. (2017). Comprehensive computational model for combining fluid hydrodynamics, light transport and biomass growth in a Taylor vortex algal photobioreactor: Eulerian approach. *Algal Research, 24*, 1-8.
32. Qiang, H., & Richmond, A. (1996). Productivity and photosynthetic efficiency of Spirulina platensis as affected by

light intensity, algal density and rate of mixing in a flat plate photobioreactor. *Journal of Applied Phycology, 8*, 139-145.
33. Baroni, É. G., Yap, K. Y., Webley, P. A., Scales, P. J., & Martin, G. J. O. (2019). The effect of nitrogen depletion on the cell size, shape, density and gravitational settling of Nannochloropsis salina, Chlorella sp. (marine) and Haematococcus pluvialis. *Algal Research, 39.*
34. Acien, F. G., Fernandez, J. M., Magan, J. J., & Molina, E. (2012). Production cost of a real microalgae production plant and strategies to reduce it. *Biotechnol Adv, 30*(6), 1344-1353.
35. Pegallapati, A. K., Arudchelvam, Y., & Nirmalakhandan, N. (2012). Energy-efficient photobioreactor configuration for algal biomass production. *Bioresour Technol, 126,* 266-273.
36. Gómez-Pérez, C. A., Espinosa, J., Montenegro Ruiz, L. C., & van Boxtel, A. J. B. (2015). CFD simulation for reduced energy costs in tubular photobioreactors using wall turbulence promoters. *Algal Research, 12*, 1-9.
37. Chen, B., Wan, C., Mehmood, M. A., Chang, J. S., Bai, F., & Zhao, X. (2017). Manipulating environmental stresses and stress tolerance of microalgae for enhanced production of lipids and value-added products-A review. *Bioresour Technol, 244*(Pt 2), 1198-1206.
38. Beal, C. M., Gerber, L. N., Thongrod, S., Phromkunthong, W., Kiron, V., Granados, J., . . . Huntley, M. E. (2018). Marine microalgae commercial production improves sustainability of global fisheries and aquaculture. *Sci Rep, 8*(1), 15064.
39. Sánchez Mirón, A., García Camacho, F., Contreras Gómez, A., Grima, E. M., & Chisti, Y. (2000). Bubble-column and airlift photobioreactors for algal culture. *AIChE Journal, 46*(9), 1872-1887.